The Crop Journal xxx (xxxx) xxx

Contents lists available at ScienceDirect

The Crop Journal

journal homepage: www.keaipublishing.com/en/journals/the-crop-journal/

Rice *ONAC016* promotes leaf senescence through abscisic acid signaling pathway involving *OsNAP*

Eunji Gi [a,1], Sung-Hwan Cho [a,1], Suk-Hwan Kim [a], Kiyoon Kang [b,*], Nam-Chon Paek [a,*]

[a] *Department of Agriculture, Forestry and Bioresources, Plant Genomics and Breeding Institute, Research Institute of Agriculture and Life Sciences, Seoul National University, Seoul 08826, Republic of Korea*
[b] *Division of Life Sciences, Incheon National University, Incheon 22012, Republic of Korea*

ARTICLE INFO

Article history:
Received 3 October 2023
Revised 15 January 2024
Accepted 28 February 2024
Available online xxxx

Keywords:
Rice
ONAC016
OsNAP
Leaf senescence
Abscisic acid signaling

ABSTRACT

Senescence-induced NAC (senNAC) TFs play a crucial role in senescence during the final stage of leaf development. In this study, we identified a rice senNAC, *ONAC016*, which functions as a positive regulator of leaf senescence. The expression of *ONAC016* increased rapidly in rice leaves during the progression of dark-induced and natural senescence. The *onac016-1* knockout mutant showed a delayed leaf yellowing phenotype, whereas the overexpression of *ONAC016* accelerated leaf senescence. Notably, *ONAC016* expression was upregulated by abscisic acid (ABA), and thus detached leaves of the *onac016-1* mutant remained green much longer under ABA treatment. Quantitative RT-PCR analysis showed that *ONAC016* upregulates the genes associated with chlorophyll degradation, senescence, and ABA signaling. Yeast one-hybrid and dual-luciferase assays revealed that ONAC016 binds directly to the promoter regions of *OsNAP*, a key gene involved in chlorophyll degradation and ABA-induced senescence. Taken together, these results suggest that *ONAC016* plays an important role in promoting leaf senescence through the ABA signaling pathway involving *OsNAP*.

© 2024 Crop Science Society of China and Institute of Crop Science, CAAS. Publishing services by Elsevier B.V. on behalf of KeAi Communications Co. Ltd. This is an open access article under the CC BY-NC-ND license (http://creativecommons.org/licenses/by-nc-nd/4.0/).

1. Introduction

The process of leaf senescence is accompanied by extensive degradation of macromolecules and dramatic changes in gene expression [1]. The onset and progression of leaf senescence are finely tuned by a combination of endogenous signals mediated by phytohormones and external factors including drought, high salinity, light, nutrient starvation, and pathogen attack [1–4].

One of the best approaches to understanding the mechanisms of leaf senescence is the isolation and analysis of mutants that exhibit delayed leaf senescence [5]. To date, several genes have been identified and characterized as regulators of leaf senescence [6,7]. In Arabidopsis, the transcription of more than 40 senescence-associated transcription factors (senTFs) increases during senescence [8]. These senTFs include the plant-specific NAM/ATAF1/ATAF2/CUC2 (NAC) TFs, which are named as senescence-induced NACs (senNACs) [8]. For instance, *ORESARA1* (*ORE1*/*ANAC092*) and *AtNAP* (*ANAC029*) are positive regulators of leaf senescence [9,10]. Mutation of *ORE1* and *AtNAP* delays leaf senescence, whereas overexpression of *ORE1* and *AtNAP* promotes leaf senescence. Contrary to the positive regulation of *ORE1* and *AtNAP* on leaf senescence, *JUNGBRUNNEN1* (*JUB1*/*ANAC042*) and *VNDINTERACTING2* (*ANAC083*/*VNI2*) were identified as negative regulator of leaf senescence. Transgenic Arabidopsis plants overexpressing *JUB1* and *VNI2* delayed leaf senescence [11,12].

Among 151 rice (*Oryza sativa*) *NAC* genes (*OsNACs*) [13], several *OsNACs* were identified as *senNACs*. Especially, *OsNAP* (*Os03g21060*) is a functional ortholog of *AtNAP* [10]. OsNAP directly upregulates chlorophyll degradation genes (CDGs) such as *STAY-GREEN* (*SGR*), *Red chlorophyll catabolite reductase 1* (*RCCR1*), *NYC1*, and *NYC3*, and senescence-associated genes (SAGs) such as *Osh36*, *OsI57*, *Osh69*, and *OsI85*, thereby promoting the leaf senescence under both natural senescence (NS) and dark-induced senescence (DIS) [14]. In contrast to the upregulation of *OsNAP* in the expression of CDGs and SAGs, *ONAC106* negatively regulates their expressions [15]. Thus, the rice plants overexpressing *ONAC106* maintain chlorophyll levels much longer and delay leaf senescence during NS and DIS.

Phytohormones act as signaling molecules and regulators of various cellular processes, including leaf senescence and abiotic stress responses. Among them, abscisic acid (ABA) is a key phytohormone that mediates plant responses to environmental stress

* Corresponding authors.
E-mail addresses: kykang@inu.ac.kr (K. Kang), ncpaek@snu.ac.kr (N.-C. Paek).
[1] These authors contributed equally to this work.

https://doi.org/10.1016/j.cj.2024.02.009
2214-5141/© 2024 Crop Science Society of China and Institute of Crop Science, CAAS. Publishing services by Elsevier B.V. on behalf of KeAi Communications Co. Ltd. This is an open access article under the CC BY-NC-ND license (http://creativecommons.org/licenses/by-nc-nd/4.0/).

Please cite this article as: E. Gi, S.-H. Cho, S.-H. Kim et al., Rice *ONAC016* promotes leaf senescence through abscisic acid signaling pathway involving *OsNAP*, The Crop Journal, https://doi.org/10.1016/j.cj.2024.02.009

[1]. Leaf senescence is known to activate ABA biosynthesis pathways [16]. Increased ABA induces the expression of several CDGs and SAGs, and leaf yellowing, which are typical phenomena associated with leaf senescence [14,17]. ABA is sensed by PYRABACTIN RESISTANCE 1 (PYR1) and PYR1-LIKE (PYL) [18,19]. The ABA-bound PYLs activate sucrose nonfermenting 1-related protein kinase 2 s (SnRK2s), followed by phosphorylating transcription factors such as ABA-responsive element-binding factors (ABFs). These phosphorylated ABFs regulate the expression of ABA-responsive genes [20]. In Arabidopsis, PYL receptors consist of 14 PYL members that are highly conserved in both amino acid sequence and in functional domain structure [18,19,21]. Among them, transgenic Arabidopsis and rice overexpressing *AtPYL9* driven by the stress-inducible RD29A show enhanced drought stress tolerance and enhanced leaf senescence [22]. In rice, a total of 13 *OsPYL* genes have been identified in the genome that are homologous to Arabidopsis *AtPYL* genes. Phylogenetic analysis indicates that AtPYL9 and seven OsPYLs (OsPYL7 to 13) belong to subfamily I [23]. In silico expression carried out using the GENEVESTIGATOR database shows that expression of *OsPYL10, 11, 13* increases gradually during the development [23].

Transcription factors (TFs) control leaf senescence by mediating ABA signaling. For instance, during leaf senescence in Arabidopsis, AtNAP activates *AAO3* transcription by directly binding its promoter region, leading to ABA biosynthesis. Elevated ABA levels induce *AtNAP* expression, establishing a positive feedback mechanism. This complex loop serves to upregulate the transcription of *SGR1*, *NYC1*, *PPH*, and *PaO*, thereby promoting chlorophyll degradation and leaf senescence. In rice, ABA increases the expression of *OsNAP*. However, *OsNAP* conversely inhibits ABA biosynthesis [14]. These reports indicate that *NAP* is functionally conserved in Arabidopsis and rice during leaf senescence. Although *NAP* genes play a crucial role in the regulation of leaf senescence, a few genes have been identified as upstream regulators. In rice, *ONAC106*, *OsNAC109*, and *OsMYB102* negatively regulate the expression of *OsNAP*, while *ONAC096*, *OsWRKY5*, and *OsERF101* act as positive regulators of *OsNAP* [15,16,24–27].

In this study, we identified and characterized the rice senNAC TF ONAC016 (*Os01g01430*), which functions as a positive regulator of leaf senescence. The *ONAC016* transcripts increased during leaf senescence process and in response to ABA treatment. Leaves of the *onac016-1* mutant retained green much longer under NS and DIS conditions, whereas overexpression of *ONAC016* resulted in an accelerated senescence phenotype. By qRT-PCR analysis, we found that *ONAC016* upregulates the expression of several CDGs (*SGR*, *NYC1*, *NYC3*, *NYC4*, *OsNOL*, and *RCCR1*) and SAGs (*OsNAP* and *OsI85*). Furthermore, we observed an upregulation of ABA signaling genes (*OsABI5* and *OsPYL9*) upon *ONAC016* overexpression. The transient *in vivo* binding assays revealed that *ONAC016* enhances the expression of *OsNAP* by directly binding to its promoter region. Taken together, our results demonstrate that *ONAC016* regulates leaf senescence via *OsNAP*-mediated senescence pathways.

2. Materials and methods

2.1. Plant materials and growth conditions

The T-DNA insertion knockout mutant of *ONAC016* (PFG_3A-09456; *onac016-1*) was obtained from Crop Biotech Institute at Kyung Hee University, Republic of Korea [28,29]. The *Oryza sativa japonica* cultivar 'Dongjin' (parental line) was used as WT. Rice plants were grown in the paddy field under natural long-day (NLD) conditions ($\geq$ 14 h sunlight/day, 37°N latitude) in Suwon, Republic of Korea, or growth chamber under long-day (LD) conditions (14 h light/10 h dark, 30 °C).

2.2. Dark incubation and hormone treatment

For dark or phytohormone treatment to detached leaves, leaves were cut from from 3-week-old plants were floated on a 3 mmol L^{-1} 2-(N-morpholino) ethanesulfonic (MES) buffer (pH 5.8) with the abaxial side up and incubated in complete darkness at 28 °C, or were floated on 3 mmol L^{-1} MES buffer containing 50 μmol L^{-1} abscisic acid (ABA), 50 μmol L^{-1} salicylic acid (SA), 50 μmol L^{-1} Methyl jasmonic acid (MeJA), 1 mmol L^{-1} a-aminocyclopropane-1-carboxylic acid (ACC), 50 μmol L^{-1} 3-indoleacetic acid (IAA), then incubated in continuous light (90 μmol m^{-2} s^{-1}) condition at 28 °C. For phytohormone treatment to rice seedlings, the sterilized WT seeds were germinated on 0.5X Murashige and Skoog (MS) phytoagar medium under continuous light at 28 °C. The 10-day-old WT seedlings were transferred to 0.5X liquid medium containing 50 μmol L^{-1} ABA, 50 μmol L^{-1} SA, 50 μmol L^{-1} MeJA, 5 mmol L^{-1} 1-aminocyclo-propane-1-carboxylic acid (ACC), 50 μmol L^{-1} gibberellic acid (GA), and 50 μmol L^{-1} indole-3-acetic acid (IAA). WT seedlings incubated in 0.5X MS liquid medium without phytohormones treatment were used as a mock control.

To test the sensitivity to ABA, the seedlings of WT, *onac016-1*, and *ONAC016*–OE1 grown for 3 d on 0.5X MS phytoagar medium were transferred to 0.5X MS liquid medium containing 0 and 5 μmol L^{-1} ABA. The root lengths of each seedling were measured after 10 d.

2.3. Plasmid construction and transformation

To generate the *ONAC016*-overexpressed transgenic rice, the full-length cDNA of *ONAC016* was amplified using the primers listed in Table S1. The amplified fragments were ligated into the pCR8/GW/TOPO TA cloning vector (Invitrogen, Carlsbad, CA, USA) and then inserted into the pMDC32 Gateway binary vector containing the 35S promoter [30]. The 35S:*ONAC016* construct was introduced into the calli generated from the mature embryos of Dongjin seeds by *Agrobacterium*-(strain LBA4404)-mediated transformation [28]. *Agrobacterium*-infected calli were transferred to 0.5X MS solid medium containing cytokinin and auxin. Plantlets regenerated from the callus were grown under continuous light conditions (90 μmol m^{-2} s^{-1}) at 30 °C.

2.4. Determination of total chlorophyll, photosynthetic activity, and ion leakage

To measure total chlorophyll contents, pigments were extracted from rice leaves incubated in complete darkness, cultivated in a paddy field, or treated with phytohormones. The extracts obtained using 80% ice-cold acetone were centrifuged at 10,000×*g* for 10 min at 10 °C and then the absorbance of the supernatants was measured at 647 and 663 nm using a UV/VIS spectrophotometer (BioTek, Winooski, VT, USA). Chlorophyll concentrations were determined by spectrophotometry as described previously [31].

To determine the photosynthetic capacity, the F_v/F_m ratio was measured using the OS-30p + instrument (Opti-Sciences, Hudson, NH, USA). The measurements were conducted in the middle part of each flag leaves from 0 to 50 d after heading (DAH).

Ion leakage was measured as described previously [32] with minor modifications. Membrane leakage was determined by measurement of electrolytes (or ions) leaking from rice leaf disc (1 cm^2). Three leaf discs from each treatment were immersed in 10 mL of 0.4 mol L^{-1} mannitol at room temperature with gentle shaking for 3 h, and conductivity of the solution was measured with a conductivity meter (CON6 METER, LaMOTTE Co., Chestertown, MD, USA) Total conductivity was determined after incubation at 85 °C for 20 min. The ion leakage rate was calculated as the percentage of initial conductivity divided by total conductivity.

2.5. Protein preparation and immunoblot analysis

Total proteins were extracted from detached leaves of rice seedlings grown for 3 weeks in the growth chamber (14 h light/10 h dark). Total proteins were separated using 12% (w/v) polyacrylamide SDS-PAGE, then electroblotted onto a Hybond-P membrane (GE Healthcare, Seoul, Republic of Korea). The photosystem proteins were detected by immunoblotting using antibodies (Lhca1, Lhcb1, PsaA, and PsaD; Agrisera antibodies, Vännäs, Sweden) at a 1:5000 dilution. And their secondary antibody (Goat anti-Rabbit IgG-HRP, 1:10000, GenDEPOT, Dawinbio, Republic of Korea) activities were visualized using the ECL system with WESTSAVE chemiluminescence detection kit (AbFRONTIER, Seoul, Republic of Korea) according to the manufacturer's protocol.

2.6. Transmission electron microscope (TEM)

TEM analysis was performed as described previously [33] with minor modifications. Segments of leaf tissues were fixed with a modified Karnovsky's fixative (2% paraformaldehyde, 2% glutaraldehyde, and 50 mmol L^{-1} sodium cacodylate buffer, pH 7.2) and washed three times with 50 mmol L^{-1} sodium cacodylate buffer (pH 7.2), at 4 °C for 10 min. The samples were post-fixed with 1% osmium tetroxide in 50 mmol L^{-1} sodium cacodylate buffer (pH 7.2) at 4 °C for 2 h, and briefly washed twice with distilled water at 25 °C. Samples were stained with bloc in 0.5% uranyl acetate at 4 °C for a minimum of 30 min, dehydrated in a gradient series of ethanol and propylene oxide, and finally embedded in Spurr's resin. After polymerization at 70 °C for 24 h, ultrathin sections were prepared with a diamond knife on an MT-X ultramicrotome (RMC Boeckeler, Tucson, AZ, USA) and mounted on Formvar-coated copper grids. The sections on the grids were stained with 2% uranyl acetate for 5 min and with Reynolds' lead citrate for 2 min at 25 °C and then examined using a JEM-1010 EX electron microscope (JEOL, Tokyo, Japan).

2.7. Quantitative reverse transcription-PCR (qRT-PCR) and semiquantitative RT-PCR

Total RNA was extracted from total rice tissues using an RNA Extraction Kit (Macrogen, Seoul, Republic of Korea) according to manufacturer instructions. 2 μg of total RNA was used for cDNA synthesis with a First-strand cDNA synthesis kit (Promega, Madison, WI, USA). 2X GoTaq qPCR Master Mix (Promega) was used for qRT-PCR reactions on the LightCycler 2.0 instrument (Roche Diagnostics, Basel, Switzerland). The rice *UBIQUITIN5* (*OsUBQ5*, Os01g22490) gene was used as an internal control for normalization. The semiquantitative PCR was performed with Ex Taq polymerase (TaKaRa Biotechniques, Shiga, Japan). The PCR products were electrophoresed on a 1% agarose gel. *OsUBQ5* was used as an equal loading control. Oligonucleotide primers are listed in Table S1.

2.8. Yeast one-hybrid assays

The coding sequences of *ONAC016* was cloned into the pGADT7 vector (Clontech, Shiga, Japan) as a prey. The promoter fragments of *OsNAP* were cloned into the *pLacZi* vector, generating *OsNAP-a::LacZi*, *OsNAP-b::LacZi*, *OsNAP-c::LacZi*, *OsNAP-d::LacZi*, *OsNAP-e::LacZi*, *OsNAP-f::LacZi*, *OsNAP-g::LacZi*, and *OsNAP-h::LacZi* reporter constructs, respectively (Clontech). The primers used are listed in Table S1. These vectors were transformed into yeast strain YM4271 using the PEG/LiAc method, and yeast cells were incubated in SD/-His/-Leu liquid medium. β-Galactosidase activity was determined by absorbance of chloramphenicol red, a hydrolysis product of chlorophenol red-β-D-galactopyranoside (CPRG), at 595 nm using a UV/VIS spectrophotometer (BioTek) according to the Yeast Protocol Handbook (Clontech).

2.9. Transient dual-luciferase assays

The *OsNAP* promoter region (−1260 to −300 bp) was cloned into the pJD301 vector, which contains the LUC reporter genes at the C-terminal region [34]. For the effector plasmids, the cDNA of *ONAC016* was cloned into the pGA3817 vector containing six copies of a MYC epitope tag [35]. Protoplasts were isolated from 10-day-old rice seedlings as previously described [36]. The constructed recombinant plasmids were co-transfected, together with 1 μg of an internal control plasmid (*pUBQ10-GUS*), into rice protoplasts as described [37]. Luciferase (LUC) activity in each cell lysate was determined using the Luciferase Assay System Kit (Promega). LUC activity was normalized against β-glucuronidase (GUS) activity derived from the internal control plasmid.

2.10. Chromatin immunoprecipitation (ChIP) assay

The *Ubipro:MYC* and *Ubipro:ONAC016-MYC* constructs (pGA3817 vector; [35]) were transfected into rice protoplasts as previously described [37]. Transfected protoplasts were suspended in protoplast incubation solution (0.5 mol L^{-1} mannitol, 20 mmol L^{-1} KCl, 4 mmol L^{-1} MES, pH 5.8) with darkness for 16 h at room temperature. The incubated protoplasts were subjected to crosslinking with 1% formaldehyde for 20 min under vacuum. Chromatin complexes were isolated, sonicated, and incubated with anti-Myc polyclonal antibody (Cell Signaling Technology, Danvers, MA, USA) as previously described [38]. The precipitated DNA was quantified by qRT-PCR (LightCycler 2.0 instrument, Roche Diagnostics, Basel, Switzerland). *OsUBQ5* was used as an internal control. Gene-specific primers are listed in Table S1.

2.11. Microarray analysis

For microarray analysis, WT and *onac016-1* plants were grown for 3 weeks in a growth chamber under LD conditions. Total RNA was extracted from detached leaves at 0 and 3 d of dark incubation (DDI) using an RNA Extraction Kit (Macrogen) according to manufacturer instructions. All microarray experiments, including data analysis, were conducted by Macrogen (Seoul, Republic of Korea). Microarray analysis was performed in two experimental replicates with two different biological replicates of the WT and *onac016-1*. The normalized values and *t*-test *P*-values from two experiment sets were averaged, and then *t*-test *P*-value < 0.05 and normalized value > 1.3 or < 0.67 were applied to DEGs.

3. Results

3.1. ONAC016 is induced by senescence

Our previous phylogenetic analysis showed that *ONAC016* (*Os01g01430*) is closely clustered with *OsNAP* (*Os03g21060*) and *AtNAP* (*At1g69490*) [24], which have been characterized as important regulators for leaf senescence in rice and Arabidopsis [10,14]. Thus, *ONAC016* may be relevant for the regulation of leaf senescence. To determine whether *ONAC016* responds to leaf senescence, we examined the expression profiles of *ONAC016* during dark-induced senescence (DIS) and natural senescence (NS) conditions. The rice leaves were detached from wild type (WT; *japonica* cultivar 'Dongjin') grown for 3 weeks in the growth chamber under long day (LD) conditions (14 h light at 30 °C/10 h dark at 28 °C). The detached leaves were incubated in a 3 mmol L^{-1} 2-(N-morpholino) ethanesulfonic acid (MES) buffer (pH 5.8) under com-

plete darkness at 28 °C. The qRT-PCR analysis showed that *ONAC016* dramatically increased after 2 d of dark incubation (DDI) (Fig. 1A). In addition, we monitored the changes in *ONAC016* transcript levels in the WT leaves grown in the paddy field (37°N latitude, Suwon, Republic of Korea) under natural long day (NLD) conditions (> 14 h light per day). Although *ONAC016* transcript levels were lower before heading, they increased dramatically after heading (Fig. 1B). Consistent with the result, *ONAC016* transcripts were detected at higher levels from the top in the yellowing sector of flag leaves than the bottom in the green sectors of these leaves (Fig. 1C). We investigated the tissue-specific expression of *ONAC016* in the rice tissues detached from WT plants grown in the paddy field at 94 d after seeding (DAS, before heading) and 120 DAS (after heading). The qRT-PCR analysis showed that, although *ONAC016* is widely expressed in rice tissues (flag leaf, FL; leaf blade, LB; leaf sheath, LS; panicle, PN; root, RT; tiller base, TB), it was highly expressed in leaf organs (FL, LB, LS) at 120 DAS (Fig. 1D). Taken together, these results suggest that *ONAC016* may regulate leaf senescence.

3.2. Loss-of-function mutation of ONAC016 delays leaf senescence

To elucidate the roles of *ONAC016* in leaf senescence, we obtained a T-DNA insertion knockout mutant (PFG_3A-09456: *onac016-1*) from the RiceGE database (https://signal.salk.edu/cgi-bin/RiceGE). In addition, transgenic rice plants overexpressing *ONAC016* were generated, resulting in three individual lines (*ONAC016*-OE1, OE2, and OE3). The *onac016-1* mutant harbored a T-DNA fragment in the second exon of *ONAC016* (Fig. 2A) and the *ONAC016*-OEs contained the *ONAC016* cDNA under the control of the 35S promoter. To confirm the effect of T-DNA insertion and *ONAC016* overexpression on the accumulation of *ONAC016* transcripts, we performed semi-quantitative RT-PCR and qRT-PCR analysis of the leaves of WT, *onac016-1*, and *ONAC016*-OEs seedlings grown under LD conditions in the growth chamber for three weeks. The *ONAC016* transcripts were completely absent in *onac016-1* mutant, whereas *ONAC016*-OEs showed high levels of *ONAC016* transcripts compared to WT (Figs. 2B, S1A). To compare the progression of leaf senescence among WT, *onac016-1*, and *ONAC016*-OEs during DIS, detached leaves of rice plants grown under LD conditions in the growth chamber for three weeks were incubated in a 3 mmol L^{-1} MES buffer (pH 5.8) under complete dark conditions at 28 °C. While the *ONAC016*-OEs leaves became yellowing at 2 DDI, the *onac016-1* leaves maintained the green color until 3 DDI (Figs. 2C, S1B). Consistent with visible phenotypes, the chlorophyll (Chl) contents of *ONAC016*-OEs decreased sharply at 2 DDI compared to WT, whereas *onac016-1* retained similar Chl contents to WT at 2 and 3 DDI (Figs. 2D, S1C). In addition, we compared the chloroplast structure of three-week-old WT and *onac016-1* leaves at 0 and 3 DDI using transmission electron microscopy. Both WT and *onac016-1* leaves have an intact chloroplast structure at 0 DDI (Fig. S2A). However, at 3 DDI, the thylakoids of *onac016-1* chloroplasts retained their grana structures, whereas those of WT chloroplasts were almost degraded (Fig. S2A). We then examined the levels of photosynthetic proteins by immunoblotting with antibodies against photosystem I (PSI) complex subunits (Lhca1 and PsaA) and photosystem II (PSII) complex subunits (Lhcb1 and PsbD) in the WT and *onac016-1* leaves at 0 and 3 DDI. The

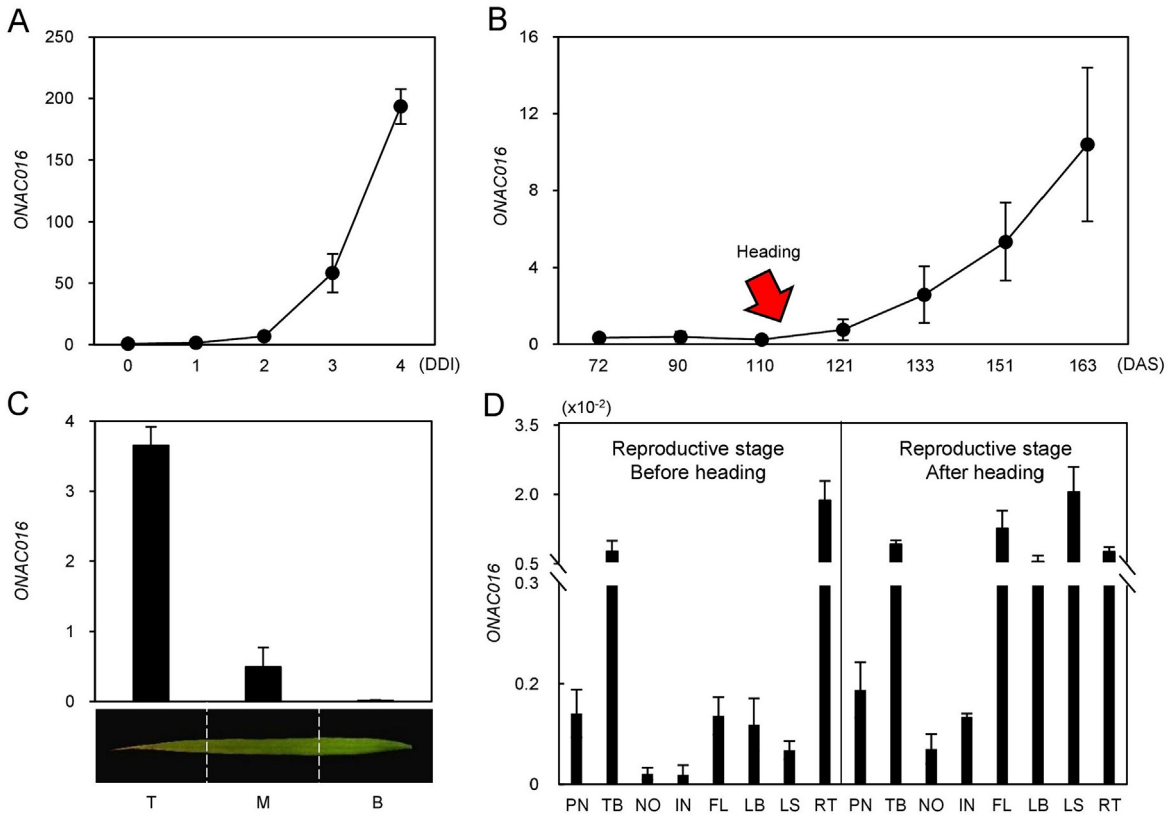

Fig. 1. Expression profiles of *ONAC016*. (A) *ONAC016* expression gradually increased in detached leaves of *japonica* cultivar 'Dongjin' (hereafter wild type; WT) seedlings grown for 3 weeks in a growth chamber under long-day (LD) condition (14 h light/10 h dark) were subjected to complete darkness in 3 mmol L^{-1} MES (pH 5.8) at 28 °C. DDI, day(s) of dark incubation. (B) WT plants were grown in the paddy field under natural long day (NLD) (≥14 h light/day). Red arrow indicated the heading date at 113 d after sowing (DAS). (C) Expression of *ONAC016* measured in different sectors of flag leaves at 106 DAS. T, tip; M, middle; B, bottom. (D) *ONAC016* was differentially expressed in rice tissue detached from WT plants at 94 DAS (before heading) and 120 DAS (after heading). PN, panicle; NO, node; IN, internode; FL, flag leave; RT, root; LB, leaf blade; LS, leaf sheath; TB, tiller base. *ONAC016* mRNA levels were determined by qRT-PCR analysis and normalized using the *OsUBQ5* (*Os01g22490*).

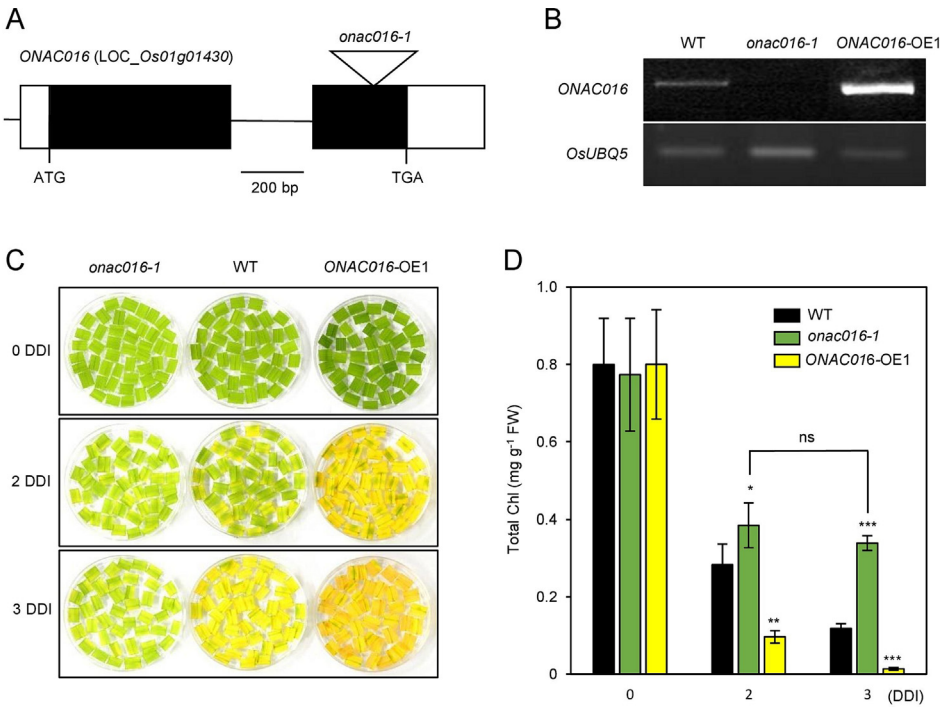

Fig. 2. The *onac016-1* mutant delayed leaf yellowing during dark-induced senescence. (A) Schematic diagram depicting the positions of T-DNA insertion. Black and white bars represent exons and untranslated regions, respectively. Open triangle indicates the location of the T-DNA insertion (*onac016-1*, PFG_1B-15010). Black line represents the intron. (B) Verification of *onac016-1* mutant and *ONAC016*-overexpressed transgenic plants (*ONAC016*-OE1) by using semi-quantitative RT-PCR analysis. Total RNA was isolated from leaves of rice seedlings grown for 3 weeks in a growth chamber under long-day (LD) condition. *OsUBQ5* (*Os01g22490*) was used as a loading control. (C, D) Detached leaves of WT, *onac016-1*, and *ONAC016*-OE1 plants grown in growth chamber under LD conditions were incubated in 3 mmol L^{-1} MES buffer (pH 5.8) with the abaxial side up at 28 °C under complete darkness. The leaf yellowing phenotype (C) and total chlorophyll (Chl) (D) were determined 0, 2, and 3 d of dark incubation (DDI). Asterisks on *onac016-1* and *ONAC016*-OE1 indicate statistically significant differences from WT, as determined by Student's *t*-test (*, $P < 0.05$; **, $P < 0.01$; ***, $P < 0.001$). Experiments were repeated twice with similar results. Mean and standard deviation values were obtained from the three biological repeats. FW, fresh weight; ns, not significance.

onac016-1 leaves remained significantly more photosynthetic proteins than the WT leaves during 3 DDI (Fig. S2B). To examine the efficiency of the photosynthetic apparatus, we measured the F_v/F_m ratio (a measure of the efficiency of PSII) at 0 and 3 DDI. The F_v/F_m ratio in WT leaves decreased more than that in *onac016-1* leaves (Fig. S2C). We also found that ion leakage rate, a typical indicator of cell membrane integrity, was significantly reduced in *onac016-1* leaves compared with WT leaves at 9 DDI (Fig. S2D). These results suggest that loss-of-function of *ONAC016* delays leaf senescence by preventing chlorophyll degradation and persisting cell membrane integrity.

To determine whether *ONAC016* affects leaf yellowing during NS, we observed the senescence phenotypes of WT, *onac016-1*, and *ONAC016*-OE1 plants. These plants were grown in the paddy field under NLD conditions and flowered simultaneously in 2022 (Fig. 3A). There was no obvious phenotypic difference in leaf greenness between WT, *onac016-1*, and *ONAC016*-OE1 up to the heading stage (Fig. 3B). However, after heading, *onac016-1* leaves retained the green color, whereas *ONAC016*-OE1 accelerated leaf yellowing compared to WT leaves (Fig. 3B). Consistent with these observations, total Chl levels were significantly higher in *onac016-1* and lower in *ONAC016*-OE1 compared to WT after 30 d after heading (DAH) (Fig. 3C). To examine whether delayed leaf senescence is associated with increased photosynthetic efficiency (PSII efficiency), we measured the F_v/F_m ratio on the flag leaves of WT, *onac016-1*, and *ONAC016*-OE1 during NS. After 30 DAH, *onac016-1* leaves exhibited relatively higher F_v/F_m values than WT leaves, while *ONAC016*-OE1 showed lower F_v/F_m values compared to WT (Fig. 3D). These consistent results for heading date, total Chl, and F_v/F_m were investigated within the same paddy field in 2021 (Fig. S3). Taken together, these results indicate that *ONAC016* affects the progression of leaf senescence under both DIS and NS conditions.

3.3. onac016-1 mutants are insensitive to abscisic acid

Leaf senescence is primarily regulated by plant age, but its progression is influenced by phytohormones [39]. In particular, ABA promotes leaf senescence by activating senescence-associated regulatory pathways [40,41]. To determine whether *ONAC016* responds to phytohormones, we examined the expression patterns of *ONAC016* in response to ABA, MeJA, ACC, GA, and IAA using qRT-PCR. After 12 h of treatments, *ONAC016* expression significantly increased up to approximately 5-fold in ABA-treated WT seedlings compared to the mock control (Fig. 4A), suggesting that *ONAC016* mainly mediates ABA-regulated leaf senescence. To confirm this observation, we tested the effects of phytohormones on detached leaves of WT, *onac016-1*, and *ONAC016*-OE1. Detached leaves from WT seedlings were incubated in a 3 mmol L^{-1} MES buffer without phytohormones as a mock control. The progress of leaf yellowing was then monitored. Compared to the mock control, WT leaves showed a yellow color at 4 d of ABA treatment (DT). However, the leaves of *onac016-1* maintained their green pigment much higher when compared to WT at 4 DT of ABA (Fig. 4B). As predicted, the *ONAC016*-OE1 leaves displayed early yellowing at 2 DT compared to the mock control (Fig. 4B). Consistent with these results, the total Chl content of WT leaves was significantly reduced by ABA treatment compared to the mock control (Fig. 4B). In particular, the total Chl contents were higher in *onac016-1* and lower in *ONAC016*-OE1 than in WT under ABA treatment (Fig. 4C). The presence of other phytohormones had no impact on the progression of leaf yellowing or the changes of Chl content compared to the mock

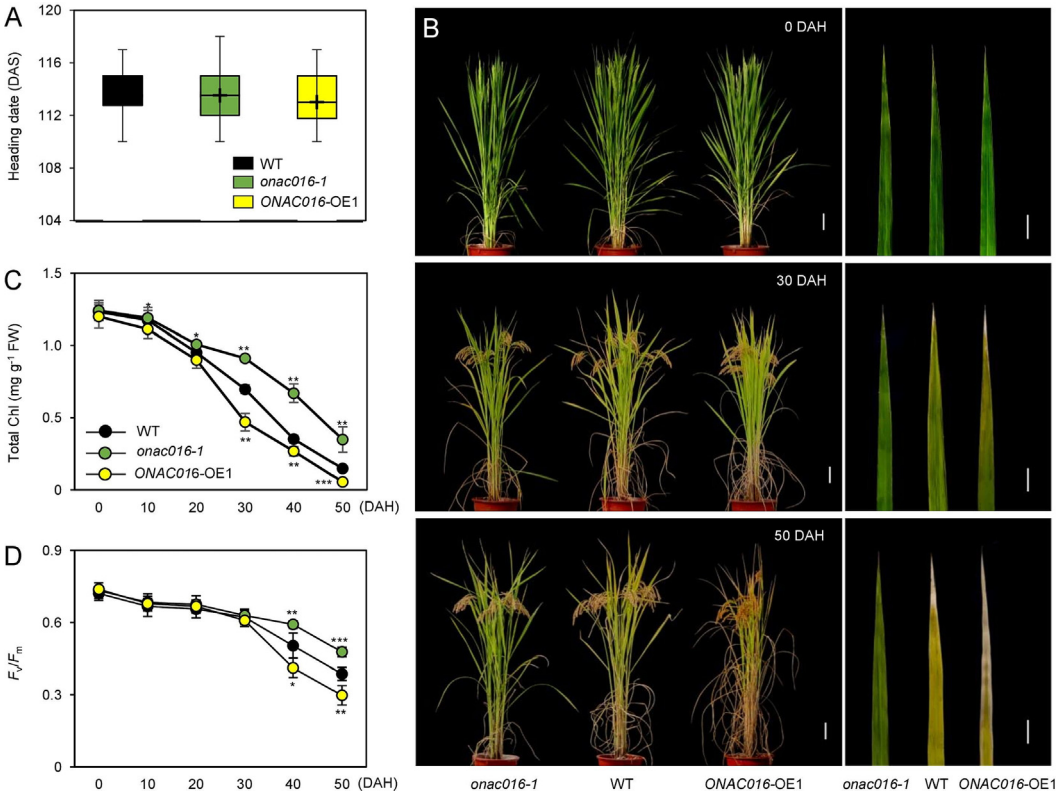

Fig. 3. The *onac016-1* mutant delayed leaf senescence during natural senescence in the year 2022. (A–D) WT, *onac016-1,* and *ONAC016*-OE1 plants grown in the paddy field under natural long day (NLD) conditions (≥14 h light/day). (A) Heading date. (B) The whole rice plants were transferred to each pot at 0, 30, and 50 d after heading (DAH). The leaf yellowing phenotype of rice plants was observed at 0, 30, and 50 DAH. The left three panels were the phenotype of whole plants and the right three panels were the phenotype of flag leaves. Scale bars, 20 cm (whole plants) and 2 cm (flag leaves). (C, D) Changes in total chlorophyll (Chl) contents (C) and photosynthetic capacity (F_v/F_m) (D) of flag leaves were determined every 10 d from 0 to 50 DAH. Mean and standard deviation values were obtained from 10 plants. Asterisks on *onac016-1* and *ONAC016*-OE1 indicate statistically significant differences from WT, as determined by Student's *t*-test (*, $P < 0.05$; **, $P < 0.01$; ***, $P < 0.001$). Box-and-whisker plots show max and min, 25–75th percentiles (box), and median (center line). DAS, days of seeding; FW, fresh weight.

control (Fig. S4). In addition, since ABA inhibits root development [42,43], we measured the root lengths of WT, *onac016-1*, and *ONAC016*-OE1 plants under ABA treatment. The results showed that, compared to the WT, the root lengths are longer and shorter in *onac016-1* and *ONAC016*-OE1, respectively at 5 μmol L^{-1} ABA (Fig. S5). These results suggest that *ONAC016* facilitates leaf senescence in response to ABA signaling.

3.4. ONAC016 positively regulates the expression of CDGs, SAGs, and ABA signaling genes

To identify the underlying mechanisms of *ONAC016* on leaf senescence, we conducted Affymetrix whole-genome microarray analysis to compare the transcriptomes in detached leaves of WT and *onac016-1* at 0 and 3 DDI as shown in Fig. 2. The threshold for significantly differentially expressed genes (DEGs) was set at $\log_2$ fold change (FC) greater than 1.3 or less than 0.67 and adjusted $P < 0.05$, resulting in 2929 DEGs in *onac016-1* mutant compared to WT (Dataset S1). Gene Ontology (GO) analysis revealed that the majority of the 2929 DEGs were associated with metabolic processes of carbohydrate, lipid, nucleotide, amino acids, as well as involved in vital signal transduction (Table S2). In addition, we identified that some chlorophyll degradation genes (CDGs) and senescence-associated genes (SAGs) were downregulated in *onac016-1* at both 0 and 3 DDI (Table S3). Using qRT-PCR analysis, the expression CDGs and SAGs were investigated in the detached leaves of WT, *onac016-1*, and *ONAC016*-OE1 during DIS as shown in Fig. 2. The CDGs and SAGs encode the chlorophyll catabolic enzymes (SGR, [5]; OsRCCR1, [44]; NYC1 and NOL, [45]; NYC3, [46], NYC4, [47]) and fatty acid metabolism-associated protein (OsI85, [48]). The qRT-PCR analysis showed that the expression of those genes significantly decreased in *onac016-1* at 3 DDI, but increased in *ONAC016*-OE1 at 2 DDI compared to WT (Fig. 5A–G). In addition, we further measured the transcript levels of ABA signaling genes such as *OsABI5*, *OsPYL8*, Os*PYL9*, *OsPYL10*, and *OsPYL11* in the detached leaves of WT, *onac016-1*, and *ONAC016*-OE1. Among them, the expression of *OsABI5* and *OsPYL9* decreased in *onac016-1* and increased in *ONAC016*-OE1 at 3 DDI (Fig. 5H, I). However, there was no significant difference in the expression of *OsPYL8*, *OsPYL10*, and *OsPYL11* during DIS (Fig. S6). These results suggest that ONAC016 promotes leaf senescence through chlorophyll degradation and ABA signaling.

3.5. ONAC016 binds to the OsNAP promoter regions

Since OsNAP serves as a positive regulator for leaf senescence [14], we further examined the expression of *OsNAP* in the detached leaves of *onac016-1* and *ONAC016*-OE1 during DIS. Transcript levels of *OsNAP* were significantly downregulated in *onac016-1* at 3 DDI, whereas they were upregulated in *ONAC016*-OE1 at 2 DDI compared to WT (Fig. 6A). To investigate whether ONAC016 directly activates the *OsNAP* transcription, we conducted the luciferase (LUC), yeast one-hybrid (Y1H) and chromatin immunoprecipitation (ChIP) assays. For the LUC assay, the promoter region of *OsNAP* containing −300 bp to −1200 bp from the start codon (red horizontal line) was fused with the *LUC* reporter gene (Fig. 6B, C). LUC activity in rice protoplasts harboring the *proOsNAP::LUC* plasmid was significantly enhanced when co-transfected with the *Ubi::ONAC016-MYC* plasmid, compared to co-transfection with the *Ubi::MYC* plasmid (Fig. 6D). Next, we examined the binding activity of

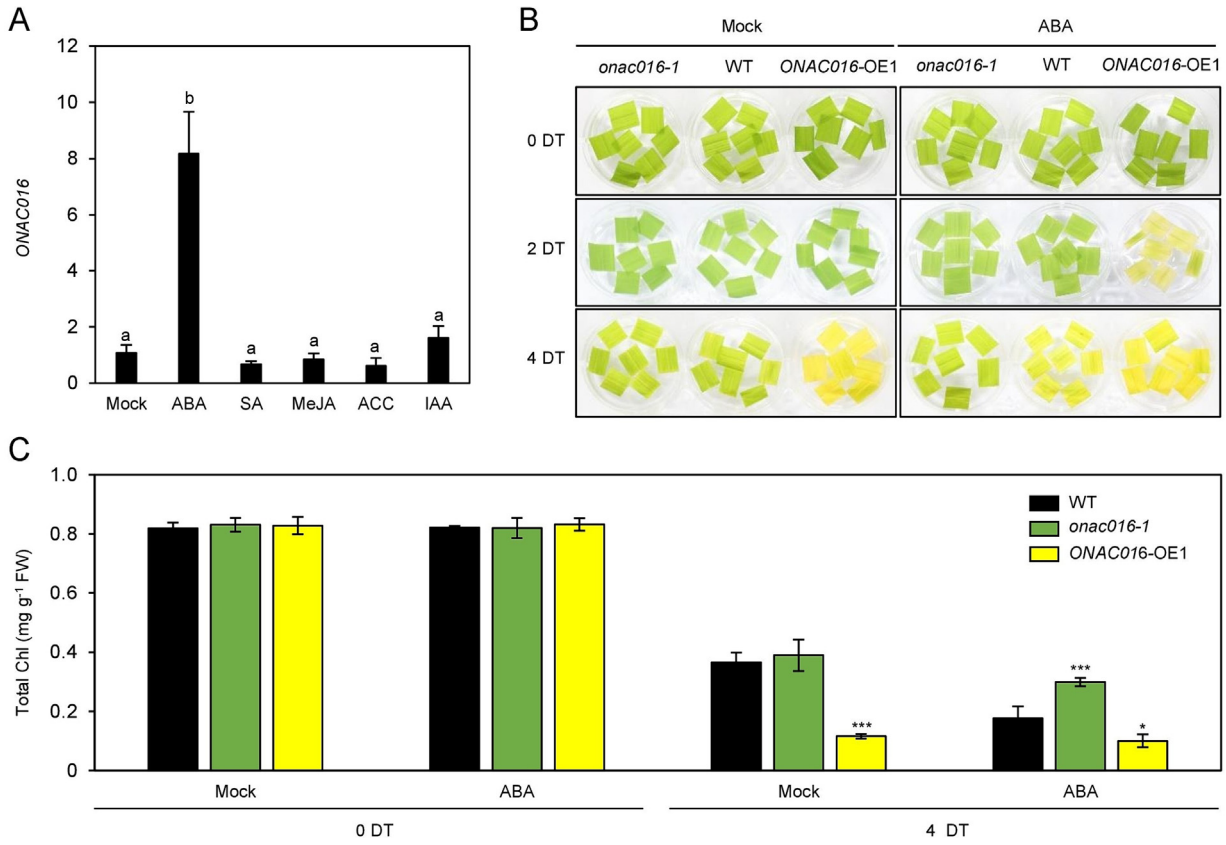

Fig. 4. The *ONAC016* mutation reduces the sensitivity to ABA. (A) Expression patterns of *ONAC016* in response to diverse phytohormones. The 10-day-old WT seedlings grown on 0.5X MS phytoagar medium at 28 °C under continuous light conditions were transferred to 0.5X MS liquid medium containing 50 μmol L^{-1} abscisic acid (ABA), 50 μmol L^{-1} salicylic acid (SA), 50 μmol L^{-1} methyl jasmonic acid (MeJA), 1 mmol L^{-1} 1-aminocyclopropane-1-carboxylic acid (ACC), and 50 μmol L^{-1} 3-indoleacetic acid (IAA). Seedlings incubated in 0.5X MS liquid medium without phytohormones were used as a mock control. Total RNA was isolated from the leaves at 12 h of treatment. Different letters indicate significantly different values according to a one-way ANOVA and Duncan's least significant rage test ($P < 0.05$). (B, C) Detached leaves of 3-week-old WT, *onac016-1*, and *ONAC016*-OE1 plants grown in the growth chamber under LD conditions were incubated in 3 mmol L^{-1} MES buffer (pH 5.8) containing 50 μmol L^{-1} ABA at 28 °C under continuous light. Detached leaves incubated in 3 mmol L^{-1} MES buffer (pH 5.8) without ABA were used as a mock control. (B) The phenotypes of WT, *onac016-1*, and *ONAC016*-OE1 were observed at 0, 2, and 4 d after treatment (DT). (C) Total chlorophyll (Chl) contents were measured at 0 and 4 DT ($n = 7$). Asterisks on *onac016-1* and *ONAC016*-OE1 indicate statistically significant differences from WT, as determined by Student's *t*-test (*, $P < 0.05$; ***, $P < 0.001$). FW, fresh weight.

ONAC016 to the *OsNAP* promoter by Y1H assays. The results showed that ONAC016 binds directly to the *OsNAP*-b, c, d, e, and f promoter regions, but did not bind to *OsNAP*-a, g, and h promoter regions (Fig. 6E). Further ChIP assays also confirmed that ONAC016 binds to the amplicon-B and C regions of the *OsNAP* promoter in *planta*, but it did not bind to amplicon-A region (Fig. 6F). These results demonstrate that *ONAC016* functions as an upstream activator of *OsNAP* transcription through direct binding to its promoter.

3.6. Mutation of ONAC016 decreases grain yield

To determine whether *ONAC016* affects grain yield, the WT, *onac016-1*, and *ONAC016*-OE1 plants were cultivated in the paddy field (37°N latitude, Suwon, Republic of Korea) under NLD conditions. Several agronomic traits including plant height, panicle length, number of panicles, number of branches per panicle, number of grains per panicle, fertility, and 1000-grain weight were investigated (Table 1). Among them, the number of panicles, fertility, and 1000-grain weight exhibited significant alteration in *onac016-1* and *ONAC016*-OE1 compared to WT, resulting in grain yield reduction in *onac016-1* and grain yield induction in *ONAC016*-OE1 (Tables 1, S4). Interestingly, although the *ONAC016* mutation exhibited delayed senescence during NS (Fig. 3), grain yield was reduced in *onac016-1* mutant.

We thus investigated the expression levels of genes in regulating panicle number, fertility, and 1000-grains weight; rice tillering (*MONOCULM1* (*MOC1*) [49]; *FLORAL ORGAN NUMBER1* (*FON1*) [50]; *LAX PANICLE2* (*LAX2*) [51]), grain weight (rice sugar efflux transporter (*OsSWEET4*) [52]; *FLOURY ENDOSPERM7* (*FLO7*) [53]; *FLOURY ENDOSPERM16* (*FLO16*) [54]; rice *PYRUVATE KINASE* (*OsPK2*) [55]) and fertility (rice *GAMETE CELLS DEFECTIVE1* (*OsGCD1*) [56]; *ENDOSPERMLESS1* (*ENL1*) [57]; *TDR INTERACTING PROTEIN3* (*TIP3*) [58]; rice *LEAKED AND DELAYED DEGRADED TAPETUM1* (*OsLDDT1*) [59]). The qRT-PCR analysis showed that expression of these genes was increased and decreased in *ONAC016*-OE1 and *onac016-1*, respectively, compared to the WT (Fig. S7). These results suggest that *ONAC016* is involved in the regulation of possible pathways related to yield components.

4. Discussion

4.1. ONAC016 promotes OsNAP-induced leaf senescence

In this study, we identified a potential role of ONAC016 as an upstream positive regulator of *OsNAP*. Transcription levels of *ONAC016* and *OsNAP* increased in senescing leaves (Fig. 1, [14]). These observations indicated the temporal and spatial concurrences between *ONAC016* and *OsNAP* expression patterns. The expression of *OsNAP* is upregulated by ABA, but not by other phy-

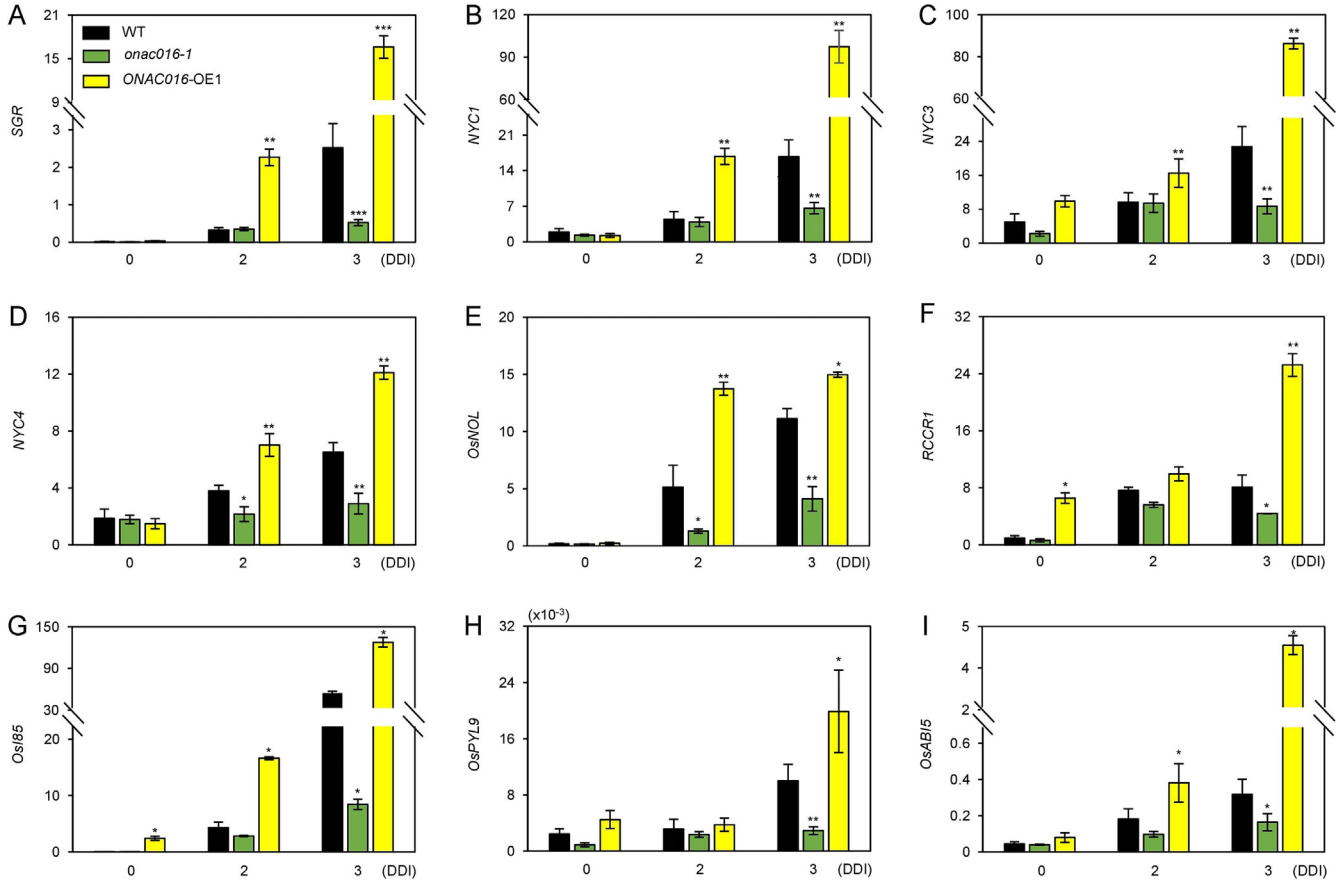

Fig. 5. Altered expression of senescence-associated genes (SAGs) and ABA signaling genes in *onac016-1* and *ONAC016*-OE1. The expression of SAGs (*SGR*, *NYC1*, *NYC3*, *NYC4*, *OsNOL*, *RCCR1*, and *Osl85*; (A–G) and ABA signaling genes (*OsPYL9* and *OsABI5*; H and I) were investigated in detached leaves of WT, *onac016-1*, and *ONAC016*-OE1 plants grown in the growth chamber under LD conditions. Total RNA was isolated from detached leaves at 0, 2, and 3 d of dark incubation (DDI). The transcript levels were determined by qRT-PCR and normalized to that of *OsUBQ5* (*Os01g22490*). Mean and standard deviations were obtained from at least three biological samples. Asterisks on *onac016-1* and *ONAC016*-OE1 indicate statistically significant differences from WT, as determined by Student's *t*-test (*, $P < 0.05$; **, $P < 0.01$; ***, $P < 0.001$).

tohormones, such as SA, JA, ACC, and IAA [14]. Therefore, downregulation of *OsNAP* by RNA interference (RNAi) renders the transgenic plants insensitive to ABA treatment and exhibits delayed leaf senescence [14]. Our result showed that *ONAC016* is specifically upregulated by ABA treatment and its mutations resulted in decreased sensitivity to exogenous ABA (Fig. 4). Moreover, *ONAC016* positively regulated the expression of SAGs and CDGs, which were directly regulated by *OsNAP*. Finally, the binding assays indicated that ONAC016 promoted chlorophyll degradation and leaf senescence through upregulating *OsNAP* (Fig. 6).

In Arabidopsis, many genes mediate the ABA signaling in the onset and progression of leaf senescence. For instance, AtNAP mediated ABA signaling by directly activating *SAG113*, a gene encoding a Golgi-localized protein phosphatase 2C (PP2C) family protein [40]. The bZIP TF ABA INSENSITIVE5 (ABI5) binds to the promoters of *NYE1/SGR1* and *NYC1* to promote chlorophyll degradation [60]. Here, we found that ONAC016 positively regulates the expression of *OsPYL9* and *OsABI5* (Fig. 5). OsPYL9 belongs to the same subfamily as AtPYL9 [23]. The PYLs activate ABA signaling by inhibiting PP2C [20]. *OsABI5*, a rice ortholog of ABI5, is induced by leaf senescence [45]. Thus, *ONAC016* upregulates leaf senescence through ABA signaling.

4.2. Negative effects of ONAC016 mutation on agronomic traits in rice

Delaying leaf senescence, a phenomenon known as 'stay-green', extends the period of photosynthetic activity throughout the grain filling stage, leading to an increase in crop yield. The stay-green trait can be divided into two distinct types: functional and non-functional. Functional stay-green (FSG) maintains both leaf greenness and photosynthetic competence, whereas non-functional stay-green maintains leaf greenness without delaying the progression of other aspects of senescence [6]. Therefore, FSG is an important trait for increasing crop yield [61] and mitigating yield losses under unfavorable environments such as water deficit and heat [22] stress [62]. Here, we found that *onac016-1*, although exhibiting FSG traits with prolonged photosynthetic activity during grain filling, reduced grain yield compared to WT (Table 1). In contrast, overexpression of *ONAC016* increased grain yield by increasing panicle number, fertility, and 1000-grain weight (Table S4).

Interestingly, it has shown that the combined application of ABA and sucrose synergistically enhanced rice grain yield and quality by improving the source-sink relationship [63]; rice grain yield was increased by either ABA or sucrose treatment, but a more significant enhancement was observed when ABA and sucrose were applied simultaneously. Furthermore, when the levels of soluble sugars, starch, and non-structural carbohydrates were assessed in both leaves and grains after flowering, these compounds simultaneously decreased in leaves (a source organ) and increased in grains (a sink organ) after treatment with ABA plus sucrose [63]. The nutrient allocation involved in the source-sink relationship is important for improving yield [64], and ABA promotes source-sink transport of photoassimilates [63]. Here, we have shown that the *onac016* mutation reduces sensitivity to ABA (Fig. 4). In this context, it is plausible that *onac016-1* could disrupt the source-sink relationship. In conclusion, the FSG trait in

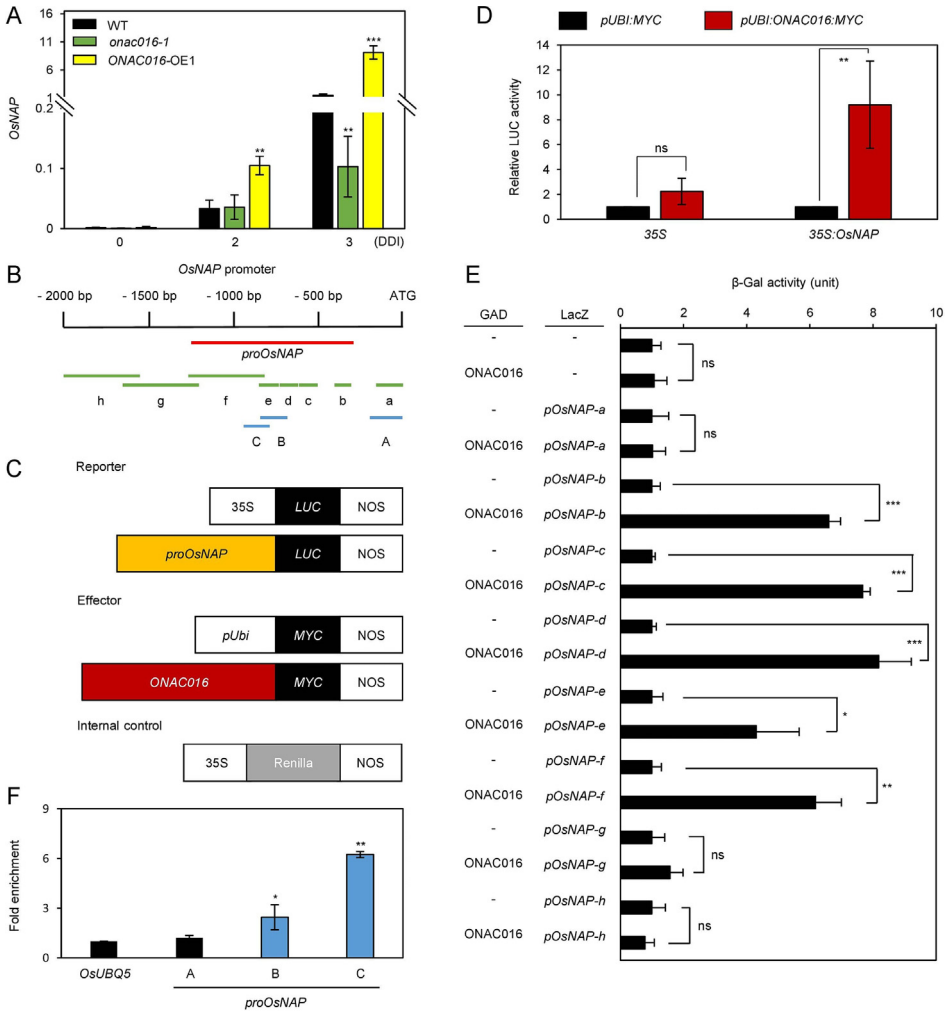

Fig. 6. ONAC016 directly activates the transcription of *OsNAP*. (A) Altered expression of *OsNAP* in *onac016-1* and *ONAC016*-OE1 in detached leaves of three-week-old WT, *onac016-1*, and *ONAC016*-OE1 plants during dark-induced senescence (DIS). Total RNA was isolated from detached leaves at 0, 2, and 3 d of dark incubation (DDI) as shown in Fig. 1A. The transcript levels were determined by qRT-PCR and normalized to that of *OsUBQ5* (*Os01g22490*). (B) The position of fragments used for the yeast one-hybrid assay (lowercase letters a–h with green lines), the transient luciferase reporter assay (red line), and the ChIP assay (uppercase letters A–C with blue lines) in the promoter region of *OsNAP*. (C) Diagrammatic illustration of the reporter, effector, and internal control constructs used in the transient luciferase reporter assay. *pUbi*, *Ubiquitin* promoter; *35S*, *35S* promoter; *LUC*, luciferase; *MYC*, myelocytomatosis oncogene. Each construct also contains the NOS terminator. (D) The activation of the *OsNAP* promoter (*proOsNAP*) by ONAC016-MYC in the protoplast transient assay. The *35S* promoter was used as a negative control. (E) β-Galactosidase activity of bait plasmids (pGADT7 and pGADT7-ONAC016) evaluated by the absorbance of chloramphenicol red, a hydrolysis product of chlorophenol red-β-D-galactopyranoside (CPRG). Empty bait (pGADT7) and prey plasmids (-) were used for negative controls. (F) ONAC016 binding affinity to the promoter regions of *OsNAP* in *planta* examined by ChIP assays. ONAC016 fused to MYC was transiently expressed in protoplasts isolated from 10-day-old WT rice seedlings. Fold enrichment of the promoter fragments was measured by immunoprecipitation with an anti-MYC antibody. *OsUBQ5* was used as the negative control. Mean and standard deviations were obtained from more than five biological repeats. Asterisks indicate statistically significant differences compared with each negative control. Student's *t*-test, (*, $P < 0.05$; **, $P < 0.01$; ***, $P < 0.001$; ns, not significance). These experiments were repeated three times with similar results.

onac016-1 mutants does not seem to correlate with an increase in grain yield.

Furthermore, we found that alteration of *ONAC016* affected the expression of genes governing rice tillering (*MOC1*, [49]; *FON1*, [50]; *LAX2*, [51]), grain weight (*OsSWEET4*, [52]; *FLO7*, [53]; *FLO16*, [54]; *OsPK2*, [55]) and fertility (*OsGCD1*, [56]; *ENL1*, [57]; *TIP3*, [58]; *OsLDDT1*, [59]) (Fig. S7). MOC1 functions as a positive regulator for rice tillers and panicle branches, and *moc1* mutation severely impairs tillering ability [49]. The loss-of-function mutation of *FON1* results in normal bud formation but defective bud outgrowth and reduced tiller number [50]. LAX2 regulates the formation of axillary meristems, and mutation of *lax2* decreases tiller number [51]. *OsSWEET4* encodes a sucrose transport protein, and *ossweet4* mutation reduces hexose transport ability, leading to diminished endosperm, hindered grouting and a reduction in grain weight [52]. *FLO7* encodes a DUF1388 protein that is specifically expressed in the endosperm periphery, and *flo7* mutant displays floury periphery phenotypes, resulting in low grain weight and quality [53]. *FLO16* encodes an NAD-dependent cytosolic malate dehydrogenase, and *flo16* mutation largely reduces ATP contents and starch synthesis-related enzyme activity, thereby decreasing 1000-grain weight [54]. *OsPK2* encodes a plastidic pyruvate kinase involved in rice endosperm starch synthesis, and *ospk2* mutation is defective in granule formation and grain filling, leading to decrease of 1000-grain weight [55]. OsGCD1 is essential for rice fertility and is required for dorsal–ventral pattern formation and endosperm free nucleus positioning [56]. *enl1* mutants have defective endosperms but carry a functional embryo [57]. *tip3* mutant displayed smaller and pale yellow anthers without mature pollen grains [58]. *OsLDDT1*, encoding a transmembrane structural DUF726 family protein, is essential for tapetum degradation and pollen formation in rice, and *osldd1* mutant aborts complete pollen

Table 1
Agronomic traits of WT, *onac016-1*, and *ONAC016*-OE1 plants in the paddy field conditions.

Trait	Genotype	2021	2022	2023
Plant height (cm)	WT (Dongjin)	107 ± 3.7	101 ± 5.2	103 ± 3.8
	onac016-1	101 ± 5.2 ^{ns}	106 ± 3.3 ^{ns}	105 ± 3 ^{ns}
	ONAC016-OE1	103 ± 3.8 ^{ns}	105 ± 1.6 ^{ns}	105 ± 1.9 ^{ns}
Panicle length (cm)	WT (Dongjin)	22 ± 1.3	21 ± 0.5	21 ± 0.7
	onac016-1	22 ± 1.0 ^{ns}	19 ± 0.8 *	20 ± 0.8 ^{ns}
	ONAC016-OE1	23 ± 1.4 ^{ns}	21 ± 0.7 ^{ns}	21 ± 1.3 ^{ns}
No. of panicles per plant	WT (Dongjin)	11 ± 1.2	10 ± 0.8	10 ± 0.7
	onac016-1	8 ± 2.2 **	7 ± 0.5 ***	6 ± 1.3 **
	ONAC016-OE1	13 ± 1.3 **	10 ± 1.3	12 ± 1.1 *
No. of branches per panicle	WT (Dongjin)	12 ± 0.9	12 ± 1.1	13 ± 1.6
	onac016-1	13 ± 1.1 ^{ns}	12 ± 0.8 ^{ns}	12 ± 1.5 ^{ns}
	ONAC016-OE1	12 ± 0.8 ^{ns}	14 ± 0.9 ^{ns}	14 ± 1.1 ^{ns}
No. of grains per panicle	WT (Dongjin)	156 ± 15.0	157 ± 10.0	156 ± 6.6
	onac016-1	159 ± 9.7 ^{ns}	138 ± 3.2 ^{ns}	157 ± 9.7 ^{ns}
	ONAC016-OE1	157 ± 15.3 ^{ns}	187 ± 4.9 ^{ns}	159 ± 12.5 ^{ns}
Fertility per plant (%)	WT (Dongjin)	91 ± 1.1	91 ± 2.3	91 ± 1.1
	onac016-1	84 ± 1.5 **	82 ± 3.0 **	84 ± 2 **
	ONAC016-OE1	93 ± 0.5 *	92 ± 1.3 ^{ns}	92 ± 0.7 *
1000-grain weight (g)	WT (Dongjin)	26.3 ± 2.8	26.8 ± 0.2	25.3 ± 0.8
	onac016-1	21.7 ± 0.8 *	22.7 ± 0.3 ***	20.7 ± 0.9 **
	ONAC016-OE1	25.8 ± 1.8 ^{ns}	29.7 ± 1.9 *	29.6 ± 1.5 *
Grain yield per plant (g)	WT (Dongjin)	39 ± 5.1	37 ± 5.3	36 ± 4.1
	onac016-1	23 ± 6.5 *	16 ± 2.5 **	17 ± 3.4 ***
	ONAC016-OE1	52 ± 7.6 *	51 ± 7.4 *	54 ± 9.1 *

Mean and standard deviations were obtained from 12 rice plants. Asterisks on *onac016-1* and *ONAC016*-OE1 indicate statistically significant differences from WT, as determined by Student's *t*-test (*, $P < 0.05$; **, $P < 0.01$; ***, $P < 0.001$; ns, not significance).

development [59]. Based on these findings, we speculated that *ONAC016* is involved in the regulation of possible pathways which affect yield components.

4.3. The possible effects of ONAC016 on plant development

TFs have the ability to influence a wide range of plant developmental processes. For instance, *ONAC106* not only negatively regulates leaf senescence but also increases salt tolerance and tiller angle [15]. *ONAC106* affects the expression of genes associated with senescence (*OsNAP, SGR,* and *NYC1*), salt stress [rice *DEHYDRATION-RESPONSIVE ELEMENT BINDING 2A* (*OsDREB2A*; [65], *OsbZIP23* [66], *OsMYB2* [67], and *STRESS-RESPONSIVE NAC1* (*SNAC1*; [68], and tiller angle *LAZY1* (*LA1*; [69]); *LOOSE PLANT ARCHITECTURE1* (*LPA1*; [70]), and *TILLER ANGLE CONTROL1* (*TAC1*; [71]) [15]. Although the rice plants overexpressing *ONAC106* showed a functional stay-green phenotype, they had reduced fertility [15]. However, *ONAC106* increased the number of grains per panicle, the number of branches per panicle, and the panicle length, ultimately increasing grain yield per plant [15]. Rice DNA-binding one zinc finger 24 (OsDof24) negatively regulates leaf senescence, exhibiting delayed leaf senescence in *OsDof24*-overexpressed rice plants [72]. Overexpression of *OsDof24* inhibited jasmonate (JA) biosynthesis during senescence by downregulating the expression of JA biosynthetic genes including *OsLOX2*, *OsLOX8*, *OsHI-LOX*, *OsAOS1*, and *OsAOS2* [72]. Impairment of JA biosynthesis or JA signaling caused severe defects in spikelet development [73]. These reports indicate that reduced endogenous JA levels in plants overexpressing *OsDof24* affect multiple aspects of plant development including leaf senescence and grain yield. These findings implied that *ONAC016* can affect not only grain yield but also diverse plant development.

In addition, our microarray results showed that the *ONAC016* mutation affects the expression of several transporter genes involving oligopeptide and nitrate transport (Datasets S2, S3). Oligopeptide transporters (OPTs) have diverse functions in nitrogen mobilization and peptide transport [74,75]. Higher plants have evolved two inorganic nitrogen (N) uptake systems: the high-affinity transporter system (HATS), which facilitates the uptake of nitrate at low nitrate concentrations, and the low-affinity transporter system (LATS) to cope with nitrate at high nitrate concentrations [76,77]. It is well established that nitrogen mobilization is closely related to grain yield during the grain-filling stage in rice [78,79]. It is plausible that *ONAC016* plays another important role in regulating nitrogen mobilization during leaf senescence. Therefore, it is worthwhile to further explore the potential regulatory mechanisms by which *ONAC016* controls nitrogen uptake and mobilization.

Gene accession numbers

Sequence data generated in this study can be found in the National Center for Biotechnology Information (NCBI) Database and Resource (https://www.ncbi.nlm.nih.gov/) under the following accession numbers: *ONAC016* (*Os01g01430*); *OsNAP* (*Os03g21060*); *SGR* (*Os09g36200*); *NYC1* (*Os01g12710*); *NYC3* (*Os06g24730*); *NYC4* (*Os07g37250*); *OsNOL* (*Os03g45194*); *RCCR1* (*Os10g25030*); *OsI85* (*Os07g34520*); *OsABI5* (*Os01g64730*); *OsPYL8* (*Os06g33640*); *OsPLY9* (*Os06g33690*); *OsPYL10* (*Os02g15640*); *OsPYL11* (*Os05g12260*); *MOC1* (*Os06g40780*); *FON1* (*Os06g50340*); *LAX2* (*Os04g32510*); *OsSWEET4* (*Os02g19820*); *FLO7* (*Os10g32680*); *FOL16* (*Os10g33800*); *OsPK2* (*Os07g08340*); *OsGCD1* (*Os01g58750*); *ENL1* (*Os04g59624*); *TIP3* (*Os03g50780*); *OsLDDT1* (*Os03g02170*); *OsUBQ5* (*Os01g22490*).

CRediT authorship contribution statement

Eunji Gi: Investigation, Data curation, Writing – original draft. **Sung-Hwan Cho:** Validation, Writing – review & editing. **Suk-Hwan Kim:** Investigation. **Kiyoon Kang:** Conceptualization, Writing – review & editing. **Nam-Chon Paek:** Conceptualization, Funding acquisition, Project administration, Writing – review & editing.

Declaration of competing interest

The authors declare that they have no known competing financial interests or personal relationships that could have appeared to influence the work reported in this paper.

Acknowlegments

This research was supported by the National Research Foundation of Korea (NRF) grant funded by the Korea government (MSIT) (2022R1A2C1091553 to Nam-Chon Paek and 2022R1F1A1075022 to Kiyoon Kang).

Appendix A. Supplementary data

Supplementary data for this article can be found online at https://doi.org/10.1016/j.cj.2024.02.009.

References

[1] P.O. Lim, H.J. Kim, H.G. Nam, Leaf senescence, Annu. Rev. Plant Biol. 58 (2007) 115–136.
[2] B. Moore, L. Zhou, F. Rolland, Q. Hall, W.H. Cheng, Y.X. Liu, I. Hwang, T. Jones, J. Sheen, Role of the *Arabidopsis* glucose sensor HXK1 in nutrient, light, and hormonal signaling, Science 300 (2003) 332–336.
[3] J. Zapata, A. Guéra, A. Esteban-Carrasco, M. Martín, B. Sabater, Chloroplasts regulate leaf senescence: delayed senescence in transgenic *ndhF*-defective tobacco, Cell Death Differ. 12 (2005) 1277–1284.
[4] Y. Sakuraba, S. Schelbert, S.Y. Park, S.H. Han, B.D. Lee, C.B. Andrès, F. Kessler, S. Hörtensteiner, N.C. Paek, STAY-GREEN and chlorophyll catabolic enzymes interact at light-harvesting complex II for chlorophyll detoxification during leaf senescence in *Arabidopsis*, Plant Cell 24 (2012) 507–518.
[5] S.Y. Park, J.W. Yu, J.S. Park, J. Li, S.C. Yoo, N.Y. Lee, S.K. Lee, S.W. Jeong, H. Soe, H. J. Koh, J.S. Jeon, Y.I. Park, N.C. Paek, The senescence-induced staygreen protein regulates chlorophyll degradation, Plant Cell 19 (2007) 1649–1664.
[6] S. Hörtensteiner, Stay-green regulates chlorophyll and chlorophyll-binding protein degradation during senescence, Trends Plant Sci. 14 (2009) 155–162.
[7] M. Kusaba, A. Tanaka, R. Tanaka, Stay-green plants: what do they tell us about the molecular mechanism of leaf senescence, Photosynth. Res. 117 (2013) 221–234.
[8] S. Balazadeh, D.M. Riaño-Pachón, B. Mueller-Roeber, Transcription factors regulating leaf senescence in *Arabidopsis thaliana*, Plant Biol. 10 (2008) 63–75.
[9] J.H. Kim, H.R. Woo, J. Kim, P.O. Lim, I.C. Lee, S.H. Choi, D. Hwang, H.G. Nam, HG, trifurcate feed-forward regulation of age-dependent cell death involving *miR164* in *Arabidopsis*, Science 323 (2009) 1053–1057.
[10] Y. Guo, S. Gan, AtNAP, a NAC family transcription factor, has an important role in leaf senescence, Plant J. 46 (2006) 601–612.
[11] A. Wu, A.D. Allu, P. Garapati, H. Siddiqui, H. Dortay, M.I. Zanor, M.A. Asensi-Fabado, S. Munne-Bosch, C. Antonio, T. Tohge, A.R. Fernie, K. Kaufmann, G.P. Xue, B. Mueller-Roeber, S. Balazadeh, *JUNGBRUNNEN1*, a reactive oxygen species-responsive NAC transcription factor, regulates longevity in *Arabidopsis*, Plant Cell 24 (2012) 482–506.
[12] S.D. Yang, P.J. Seo, H.K. Yoon, C.M. Park, The Arabidopsis NAC transcription factor VNI2 integrates abscisic acid signals into leaf senescence via the *COR/RD* genes, Plant Cell 23 (2011) 2155–2168.
[13] M. Nuruzzaman, R. Manimekalai, A.M. Sharoni, K. Satoh, H. Kondoh, H. Ooka, S. Kikuchi, Genome-wide analysis of NAC transcription factor family in rice, Gene 465 (2010) 30–44.
[14] C. Liang, Y. Wang, Y. Zhu, J. Tang, B. Hu, L. Liu, S. Ou, H. Wu, X. Sun, J. Chu, C. Chu, OsNAP connects abscisic acid and leaf senescence by fine-tuning abscisic acid biosynthesis and directly targeting senescence-associated genes in rice, Proc. Natl. Acad. Sci. U. S. A. 111 (2014) 10013–10018.
[15] Y. Sakuraba, P. Weilan, J.H. Lim, S.H. Han, Y.S. Kim, G. An, N.C. Paek, Rice ONAC106 inhibits leaf senescence and increases salt tolerance and tiller angle, Plant Cell Physiol. 56 (2015) 2325–2339.
[16] T. Kim, K. Kang, S.H. Kim, G. An, N.C. Peak, OsWRKY5 promotes rice leaf senescence via senescence-associated NAC and abscisic acid biosynthesis pathway, Int. J. Mol. Sci. 20 (2019) 4437.
[17] L.M. Weaver, S. Gan, B. Quirino, R.M. Amasino, A comparison of the expression patterns of several senescence-associated genes in response to stress and hormone treatment, Plant Mol. Biol. 37 (1998) 455–469.
[18] S.Y. Park, P. Fung, N. Nishimura, D.R. Jensen, H. Fujii, Y. Zhao, S. Lumba, J. Santiago, A. Rodrigues, T.F. Chow, S.E. Alfred, D. Bonetta, R. Finkelstein, N.J. Provart, D. Desveaux, P.L. Rodriguez, P. McCourt, J.K. Zhu, J.I. Schroeder, B.F. Volkman, S.R. Cutler, Abscisic acid inhibits type 2C protein phosphatases via the PYR/PYL family of START proteins, Science 324 (2009) 1068–1071.
[19] Y. Ma, I. Szostkiewicz, A. Korte, D. Moes, Y. Yang, A. Christmann, E. Grill, Regulators of PP2C phosphatase activity function as abscisic acid sensors, Science 324 (2009) 1064–1068.
[20] T. Furihata, K. Maruyama, Y. Fujita, T. Umezawa, R. Yoshida, K. Shinozaki, K. Yamaguchi-Shinozaki, Abscisic acid-dependent multisite phosphorylation regulates the activity of a transcription activator AREB1, Proc. Natl. Acad. Sci. U. S. A. 103 (2006) 1988–1993.
[21] J. Santiago, F. Dupeux, K. Betz, R. Antoni, M. Gonzalez-Guzman, L. Rodriguez, J. A. Márquez, P.L. Rodriguez, Structural insights into PYR/PYL/RCAR ABA receptors and PP2Cs, Plant Sci. 182 (2012) 3–11.
[22] Y. Zhao, Z. Cha, J. Gao, L. Xing, M. Cao, C. Yu, Y. Hu, J. You, H. Shi, Y. Zhu, Y. Gong, Z. Mu, H. Wang, X. Deng, P. Wang, R.A. Bressan, J.K. Zhu, BA receptor PYL9 promotes drought resistance and leaf senescence, Proc. Natl. Acad. Sci. U. S. A. 113 (2016) 1949–1954.
[23] S.K. Yadav, V.V. Santosh Kumar, R.K. Verma, P. Yadav, A. Saroha, D.P. Wankhede, B. Chaudhary, V. Chinnusamy, Genome-wide identification and characterization of ABA receptor *PYL* gene family in rice, BMC Genomics 21 (2020) 676.
[24] K. Kang, Y. Shim, E. Gi, G. An, N.C. Paek, Mutation of *ONAC096* enhances grain yield by increasing panicle number and delaying leaf senescence during grain filling in rice, Int. J. Mol. Sci. 20 (2019) 5241.
[25] W. Piao, Y. Sakuraba, N.C. Paek, Transgenic expression of rice MYB102 (OsMYB102) delays leaf senescence and decreases abiotic stress tolerance in *Arabidopsis thaliana*, BMB Rep. 52 (2019) 653–658.
[26] C. Lim, K. Kang, Y. Shim, Y. Sakuraba, G. An, N.C. Paek, Rice ETHYLENE RESPONSE FACTOR 101 promotes leaf senescence through jasmonic acid-mediated regulation of *OsNAP* and *OsMYC2*, Front. Plant Sci. 11 (2020) 1096.
[27] L. Li, Y. He, Z. Zhang, Y. Shi, X. Zhang, X. Xu, J.L. Wu, S. Tang, OsNAC109 regulates senescence, growth and development by altering the expression of senescence- and phytohormone-associated genes in rice, Plant Mol. Biol. 105 (2021) 637–654.
[28] J.S. Jeon, S. Lee, K.H. Jung, S.H. Jun, D.H. Jeong, J. Lee, C. Kim, S. Jang, K. Yang, J. Nam, K. An, M.J. Han, R.J. Sung, H.S. Choi, J.H. Yu, J.H. Choi, S.Y. Cho, S.S. Cha, S.I. Kim, G. An, T-DNA insertional mutagenesis for functional genomics in rice, Plant J. 22 (2000) 561–570.
[29] D.H. Joeng, S. An, H.G. Kang, S. Moon, J.J. Han, S. Park, H.S. Lee, K. An, G. An, T-DNA insertional mutagenesis for activation tagging in rice, Plant Physiol. 130 (2002) 1636–1644.
[30] M.D. Curtis, U. Grossniklaus, A gateway cloning vector set for high-throughput functional analysis of genes in planta, Plant Physiol. 133 (2003) 462–469.
[31] R.J. Porra, W.A. Thompson, P.E. Kriedemann, Determination of accurate extinction coefficients and simultaneous equations for assaying chlorophylls *a* and *b* extracted with four different solvents: verification of the concentration of chlorophyll standards by atomic absorption spectroscopy, Biochim. Biophys. Acta 975 (1989) 384–394.
[32] S.H. Lee, Y. Sakuraba, T. Lee, K.W. Kim, G. An, H.Y. Lee, N.C. Paek, Mutation of *Oryza sativa CORONATINE INSENSITIVE 1b* (*OsCOI1b*) delays leaf senescence, J. Integr. Plant Biol. 57 (2015) 562–576.
[33] N. Inada, A. Sakai, H. Kuroiwa, T. Kuroiwa, Three-dimensional analysis of the senescence program in rice (*Oryza sativa* L.) coleoptiles, Planta 206 (1998) 585–597.
[34] K.R. Luehrsen, J.R. de Wet, V. Walbot, Transient expression analysis in plants using firefly luciferase reporter gene, Methods Enzymol. 216 (1992) 397–414.
[35] S.R. Kim, D.Y. Lee, J.I. Yang, S. Moon, G. An, Cloning vectors for rice, J. Plant Biol. 52 (2009) 73–78.
[36] Y. Zhang, J. Su, S. Duan, Y. Ao, J. Dai, J. Liu, P. Wang, Y. Li, B. Liu, D. Feng, J. Wang, H. Wang, A highly efficient rice green tissue protoplast system for transient gene expression and studying light/chloroplast-related processes, Plant Methods 7 (2011) 30.
[37] S.D. Yoo, Y.H. Cho, J. Sheen, *Arabidopsis* mesophyll protoplasts: a versatile cell system for transient gene expression analysis, Nat. Protoc. 2 (2007) 1565–1572.
[38] A. Saleh, R. Alvarez-Venegas, Z. Avramova, An efficient chromatin immunoprecipitation (ChIP) protocol for studying histone modification in Arabidopsis plants, Nat. Protoc. 3 (2008) 1018–1025.
[39] P. Huang, Z. Li, H. Guo, New advances in the regulation of leaf senescence by classical and peptide hormones, Front. Plant Sci. 13 (2022) 923136.
[40] K. Zhang, S.S. Gan, An abscisic acid-AtNAP transcription factor-SAG113 protein phosphatase 2C regulatory chain for controlling dehydration in senescing Arabidopsis leaves, Plant Physiol. 158 (2012) 961–969.
[41] S. Gao, J. Gao, X. Zhu, Y. Song, Z. Li, G. Ren, X. Zhou, B. Kuai, ABF2, ABF3, and ABF4 promote ABA-mediated chlorophyll degradation and leaf senescence by transcriptional activation of chlorophyll catabolic genes and senescence-associated genes in *Arabidopsis*, Mol. Plant (2016) 1272–1285.
[42] S.I. Park, J.J. Kim, S.Y. Shin, Y.S. Kim, H.S. Yoon, *ASR* enhances environmental stress tolerance and improves grain yield by modulating stomatal closure in rice, Front. Plant Sci. 10 (2020) 1752.
[43] H. Fujii, J.K. Zhu, Arabidopsis mutant deficient in 3 abscisic acid-activated protein kinases reveals critical roles in growth, reproduction, and stress, Proc. Natl. Acad. Sci. U. S. A. 106 (2009) 12987–12992.
[44] Y. Tang, M. Li, Y. Chen, P. Wu, G. Wu, H. Jiang, Knockdown of *OsPAO* and *OsRCCR1* cause different plant death phenotypes in rice, J. Plant Physiol. 168 (2011) 1952–1959.
[45] Y. Sato, R. Morita, S. Katsuma, M. Nishimura, A. Tanaka, M. Kusaba, Two short-chain dehydrogenase/reductases, NON-YELLOW COLORING 1 and NYC1-LIKE, are required for chlorophyll *b* and light-harvesting complex II degradation during senescence in rice, Plant J. 57 (2009) 120–131.
[46] R. Morita, Y. Sato, Y. Masuda, M. Nishimura, M. Kusaba, Defect in non-yellow coloring 3, an alpha/beta hydrolase-fold family protein, causes a stay-green phenotype during leaf senescence in rice, Plant J. 59 (2009) 940–952.

[47] H. Yamatani, Y. Sato, Y. Masuda, Y. Kato, R. Morita, K. Fukunaga, Y. Nagamura, M. Nishimura, W. Sakamoto, A. Tanaka, M. Kusaba, *NYC4*, the rice ortholog of Arabidopsis *THF1*, is involved in the degradation of chlorophyll - protein complexes during leaf senescence, Plant J. 74 (2013) 652–662.
[48] R.H. Lee, C.H. Wang, L.T. Huang, S.C. Chen, Leaf senescence in rice plants: cloning and characterization of senescence up-regulated genes, J. Exp. Bot. 52 (2001) 1117–1121.
[49] X. Li, Q. Qian, Z. Fu, Y. Wang, G. Xiong, D. Zeng, X. Wang, X. Liu, S. Teng, F. Hiroshi, M. Yuan, D. Luo, B. Han, J. Li, Control of tillering in rice, Nature 422 (2003) 618–621.
[50] G. Shao, Z. Lu, J. Xiong, B. Wang, Y. Jing, X. Meng, G. Liu, H. Ma, Y. Liang, F. Chen, Y. Wang, J. Li, H. Yu, Tiller bud formation regulators MOC1 and MOC3 cooperatively promotes tiller bud outgrowth by activating *FON1* expression in rice, Mol. Plant 12 (2019) 1090–1102.
[51] H. Tabuchi, Y. Zhang, S. Hattori, M. Omae, S. Shimizu-Sato, T. Oikawa, Q. Qian, M. Nishimura, H. Kitano, H. Xie, X. Fang, H. Yoshida, J. Kyozuka, F. Chen, Y. Sato, *LAX PANICLE2* of rice encodes a novel nuclear protein and regulates the formation of axillary meristems, Plant Cell 23 (2011) 3276–3287.
[52] D. Sosso, D. Luo, Q.B. Li, J. Sasse, J. Yang, G. Gendrot, M. Suzuki, K.E. Koch, D.R. McCarty, P.S. Chourey, P.M. Rogowsky, J. Ross-Ibarra, B. Yang, W.B. Frommer, Seed filling in domesticated maize and rice depends on SWEET-mediated hexose transport, Nat. Genet. 47 (2015) 1489–1493.
[53] L. Zhang, Y. Ren, B. Lu, C. Yang, Z. Feng, Z. Liu, J. Chen, W. Ma, Y. Wang, X. Yu, Y. Wang, W. Zhang, Y. Wang, S. Liu, F. Wu, X. Zhang, X. Guo, Y. Bao, L. Jiang, J. Wan, *FLOURY ENDOSPERM7* encodes a regulator of starch synthesis and amyloplast development essential for peripheral endosperm development in rice, J. Exp. Bot. 67 (2016) 633–647.
[54] X. Teng, M. Zhong, X. Zhu, C. Wang, Y. Ren, Y. Wang, H. Zhang, L. Jiang, D. Wang, Y. Hao, M. Wu, J. Zhu, X. Zhang, X. Guo, Y. Wang, J. Wan, *FLOURY ENDOSPERM16* encoding a NAD-dependent cytosolic malate dehydrogenase plays an important role in starch synthesis and seed development in rice, Plant Biotechnol. J. 17 (2019) 1914–1927.
[55] Y. Cai, S. Li, G. Jiao, Z. Sheng, Y. Wu, G. Shao, L. Xie, C. Peng, J. Xu, S. Tang, X. Wei, P. Hu, *OsPK2* encodes a plastidic pyruvate kinase involved in rice endosperm starch synthesis, compound granule formation and grain filling, Plant Biotechnol. J. 16 (2018) 1878–1891.
[56] X. Huang, X. Peng, M.X. Sun, *OsGCD1* is essential for rice fertility and required for embryo dorsal-ventral pattern formation and endosperm development, New Phytol. 215 (2017) 1039–1058.
[57] T. Hara, H. Katoh, D. Ogawa, Y. Kagaya, Y. Sato, H. Kitano, Y. Nagato, R. Ishikawa, A. Ono, T. Kinoshita, S. Takeda, T. Hattori, Rice SNF2 family helicase ENL1 is essential for syncytial endosperm development, Plant J. 81 (2015) 1–12.
[58] Z. Yang, L. Sun, P. Zhang, Y. Zhang, P. Yu, L. Liu, A. Abbas, X. Xiang, W. Wu, X. Zhan, L. Cao, S. Cheng, *TDR INTERACTING PROTEIN 3*, encoding a PHD-finger transcription factor, regulates ubisch bodies and pollen wall formation in rice, Plant J. 99 (2019) 844–861.
[59] Z. Sun, K. Liu, C. Chen, D. Chen, Z. Peng, R. Zhou, L. Liu, D. He, W. Duan, H. Chen, C. Huang, Z. Ruan, Y. Zhang, L. Cao, X. Zhan, S. Cheng, L. Sun, *OsLDDT1*, encoding a transmembrane structural DUF726 family protein, is essential for tapetum degradation and pollen formation in rice, Plant Sci. 329 (2023) 111596.
[60] Y. Sakuraba, J. Jeong, M.Y. Kang, J. Kim, N.C. Paek, Phytochrome-interacting transcription factors PIF4 and PIF5 induce leaf senescence in *Arabidopsis*, Nat. Commun. 5 (2014) 4636.
[61] S.C. Yoo, S.H. Cho, H. Zhang, H.C. Paik, C.H. Lee, J. Li, J.H. Yoo, B.W. Lee, H.J. Koh, H.S. Seo, N.C. Paek, Quantitative trait loci associated with functional stay-green SNU-SG1 in rice, Mol. Cells 24 (2007) 83–94.
[62] N.M. Kamal, Y.S. Alnor Gorafi, M. Abdelrahman, E. Abdellatef, H. Tsujimoto, Stay-green trait: a prospective approach for yield potential, and drought and heat stress adaptation in globally important cereals, Int. J. Mol. Sci. 20 (2019) 5837.
[63] T. Chen, G. Li, M.R. Islam, W. Fu, B. Feng, L. Tao, G. Fu, Abscisic acid synergizes with sucrose to enhance grain yield and quality of rice by improving the source-sink relationship, BMC Plant Biol. 19 (2019) 525.
[64] P. Bai, R.Q. Bai, Y.X. Jin, Characteristics and coordination of source-sink relationships in super hybrid rice, Open Life Sci. 11 (2016) 470–475.
[65] G. Mallikarjuna, K. Mallikarjuna, M.K. Reddy, T. Kaul, Expression of OsDREB2A transcription factor confers enhanced dehydration and salt stress tolerance in rice (*Oryza sativa* L.), Biotechnol. Lett. 33 (2011) 1689–1697.
[66] Y. Xiang, N. Tang, H. Du, H. Ye, L. Xiong, Characterization of OsbZIP23 as a key player of the basic leucine zipper transcription factor family for conferring abscisic acid sensitivity and salinity and drought tolerance in rice, Plant Physiol. 148 (2008) 1938–1952.
[67] A. Yang, X. Dai, W.H. Zhang, A R2R3-type MYB gene, *OsMYB2*, is involved in salt, cold, and dehydration tolerance in rice, J. Exp. Bot. 63 (2012) 2541–2556.
[68] H. Hu, M. Dai, J. Yao, B. Xiao, X. Li, Q. Zhang, L. Xiong, Overexpressing a NAM, ATAF, and CUC (NAC) transcription factor enhances drought resistance and salt tolerance in rice, Proc. Natl. Acad. Sci. U. S. A. 106 (2006) 12987–12992.
[69] P. Li, Y. Wang, Q. Qian, Z. Fu, M. Wang, D. Zeng, B. Li, X. Wang, J. Li, *LAZY1* controls rice shoot gravitropism through regulating polar auxin transport, Cell Res. 17 (2007) 402–410.
[70] X. Wu, D. Tang, M. Li, K. Wang, Z. Cheng, Loose plant Architecture1, an INDETERMINATE DOMAIN protein involved in shoot gravitropism, regulates plant architecture in rice, Plant Physiol. 161 (2013) 317–329.
[71] B. Yu, X. Lin, H. Li, X. Li, J. Li, Y. Wang, X. Zhang, Z. Zhu, W. Zhai, X. Wang, D. Xie, C. Sun, *TAC1*, a major quantitative trait locus controlling tiller angle in rice, Plant J. 52 (2007) 891–898.
[72] Y. Shim, K. Kang, G. An, N.C. Paek, Rice DNA-binding one zinc finger 24 (OsDOF24) delays leaf senescence in a jasmonate-mediated pathway, Plant Cell Physiol. 60 (2019) 2065–2076.
[73] Q. Cai, Z. Yuan, M. Chen, C. Yin, Z. Luo, X. Zhao, W. Liang, J. Hu, D. Zhang, Jasmonic acid regulates spikelet development in rice, Nat. Commun. 5 (2014) 3476.
[74] L. Williams, A. Miller, Transporters responsible for the uptake and partitioning of nitrogenous solutes, Annu. Rev. Plant Physiol. Plant Mol. Biol. 52 (2001) 659–688.
[75] X. Zhao, J. Huang, H. Yu, L. Wang, W. Xie, Genomic survey, characterization and expression profile analysis of the peptide transporter family in rice (*Oryza sativa* L.), BMC Plant Biol. 10 (2010) 92.
[76] N.M. Crawford, D.M.G. Anthony, Molecular and physiological aspects of nitrate uptake in plants, Trends Plant Sci. 3 (1998) 389–395.
[77] N.M. Crawford, B.G. Forde, Molecular and developmental biology of inorganic nitrogen nutrition, Arabidopsis Book 1 (2002) e0011.
[78] S.G. Che, B.Q. Zhao, Y.T. Li, L. Yuan, W. Li, Z.A. Lin, S.W. Hu, B. Shen, Review grain yield and nitrogen use efficiency in rice production regions in China, J. Integr. Agric. 14 (2015) 2456–2466.
[79] J. Peng, Y. Feng, X. Wang, J. Li, G. Xu, S. Phonenasay, Q. Luo, Z. Han, W. Lu, Effects of nitrogen application rate on the photosynthetic pigment, leaf fluorescence characteristics, and yield of indica hybrid rice and their interrelations, Sci. Rep. 11 (2021) 7485.